Science Advances
AAAS

Supplementary Materials for

LEDGF/p75 promotes transcriptional pausing through preventing SPT5 phosphorylation

Chenghao Guo *et al.*

Corresponding author: Zhuojuan Luo, zjluo@seu.edu.cn; Chengqi Lin, cqlin@seu.edu.cn; Zheng Ge, zhengge@seu.edu.cn

Sci. Adv. **11**, eadr2131 (2025)
DOI: 10.1126/sciadv.adr2131

This PDF file includes:

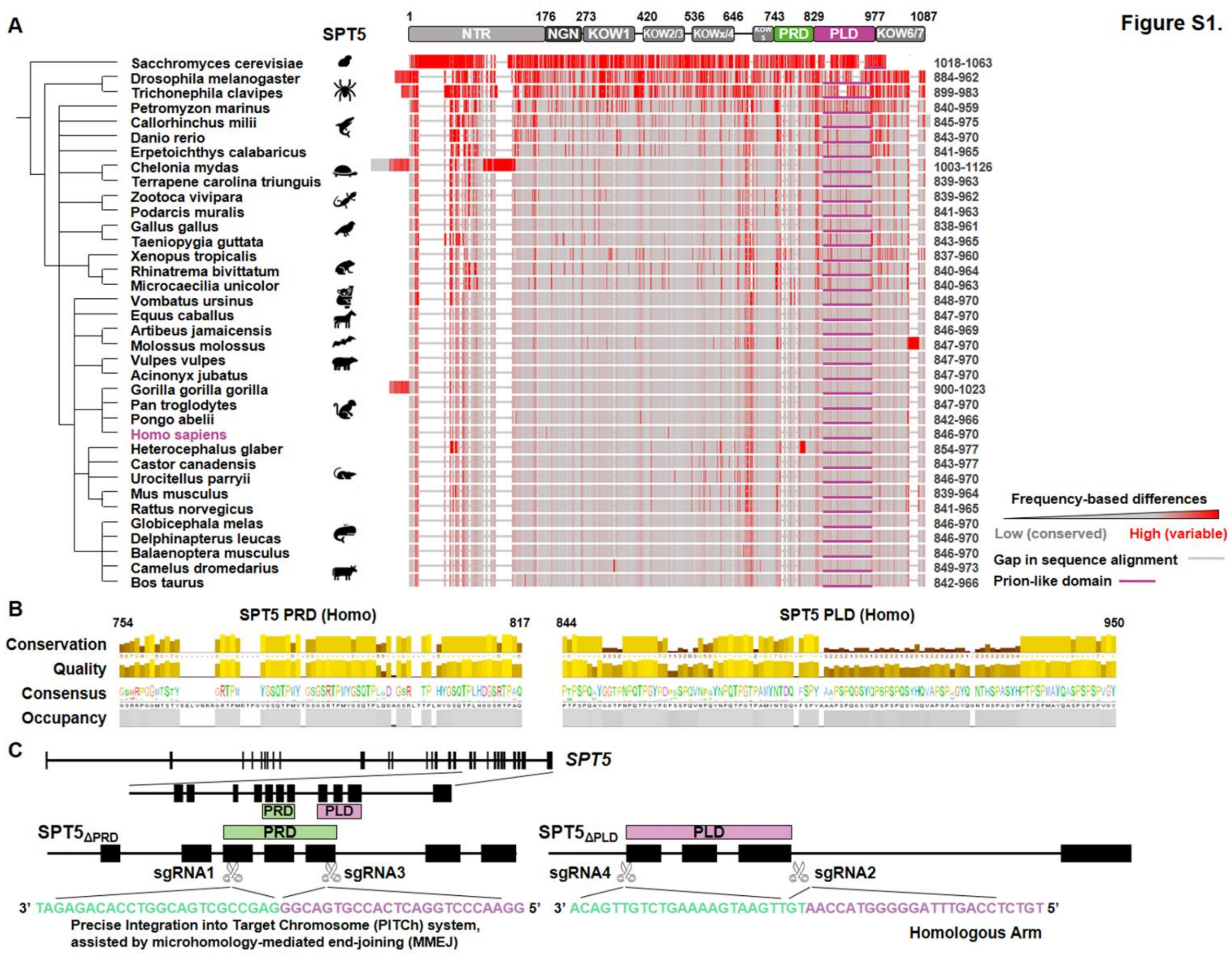

Figure S1. SPT5-CTR is conserved in metazoan.

(A) Phylogenetic tree comparing the evolution of the modular domains of SPT5. FASTA sequences were obtained for 36 representative organisms for. Organisms were grouped using the National Center for Biotechnology Information (NCBI) Taxonomy Common Tree algorithm, and the generated tree was visualized using the European Molecular Biology Laboratory (EMBL) Interactive Tree of Life (iTOL) tool. Sequences were aligned using the NCBI Cobalt algorithm using default settings, and color coding was assigned based on frequency-based differences, where red indicates highly variable regions with high frequency of mutations and gray indicates highly conserved regions with low frequency of mutations. Sequence gaps are indicated by unbroken gray lines. The violet lines indicate the PLAAC prion propensity scores. (B) The conservation analysis of PRD or PLD in SPT5-CTR. (C) Schematic representation of the positions of the sgRNAs and homologous templates used to deletion of SPT5-PRD or -PLD.

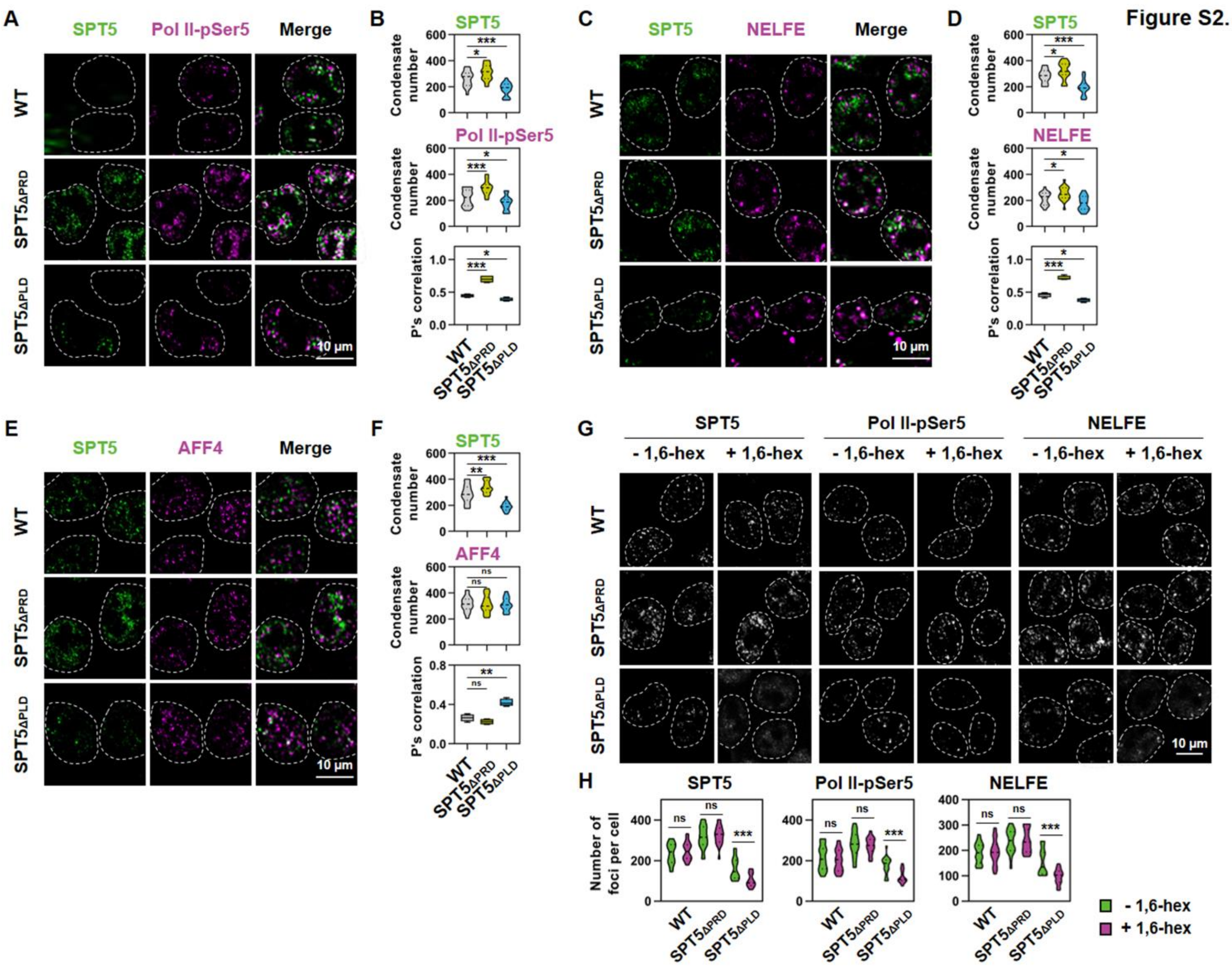

Figure S2. Adjacent PRD and PLD in SPT5 exhibit different phase separation property.

(A) Confocal images showing co-localization of Pol II-pSer5 with SPT5 in nuclear puncta in WT, $SPT5_{\Delta PRD}$, and $SPT5_{\Delta PLD}$ HCT 116 cells after serum starvation. (B) Violin plot (top and mid panel) showing the number of SPT5 and Pol II-pSer5 nuclear puncta per cell in Figure S2A. Box plots (bottom panel) showing the mean values of the Pearson correlation coefficient of co-localization ratios of SPT5 and Pol II-pSer5 in Figure S2A. (C) Confocal images showing co-localization of SPT5 with NELFE in nuclear puncta in WT, $SPT5_{\Delta PRD}$, and $SPT5_{\Delta PLD}$ HCT 116 cells. (D) Violin plot (top and mid panel) showing the number of SPT5 and NELFE nuclear puncta per cell in Figure S2C. Box plots (bottom panel) showing the mean values of the Pearson correlation coefficient of co-localization ratios of SPT5 and NELFE in Figure S2C. (E) Confocal images showing co-localization of AFF4 with SPT5 in nuclear puncta in WT, $SPT5_{\Delta PRD}$, and $SPT5_{\Delta PLD}$ HCT 116 cells after serum induction. (F) Violin plot (top and mid panel) showing the number of SPT5 and AFF4 nuclear puncta per cell in Figure S2E. Box plots (bottom panel) showing the mean values of the Pearson correlation coefficient of co-localization ratios of SPT5 and AFF4 in Figure S2E. (G) Confocal images showing that SPT5, Pol II-S5P or NELFE formed nuclear puncta in WT, $SPT5_{\Delta PRD}$, and $SPT5_{\Delta PLD}$ HCT 116 cells before and after treated with 1% 1,6-hexanediol (abbreviation as 1,6-hex) for 30 minutes in serum starvation condition. (H) Violin plot showing the number of cells containing nuclear puncta in Figure S2G. Results in Figure B, D, F, H are representative of three biological replicates, each $n > 20$. Two-tailed, unpaired Student's *t* test was performed. *$p < 0.05$, **$p < 0.01$, ***$p < 0.001$.

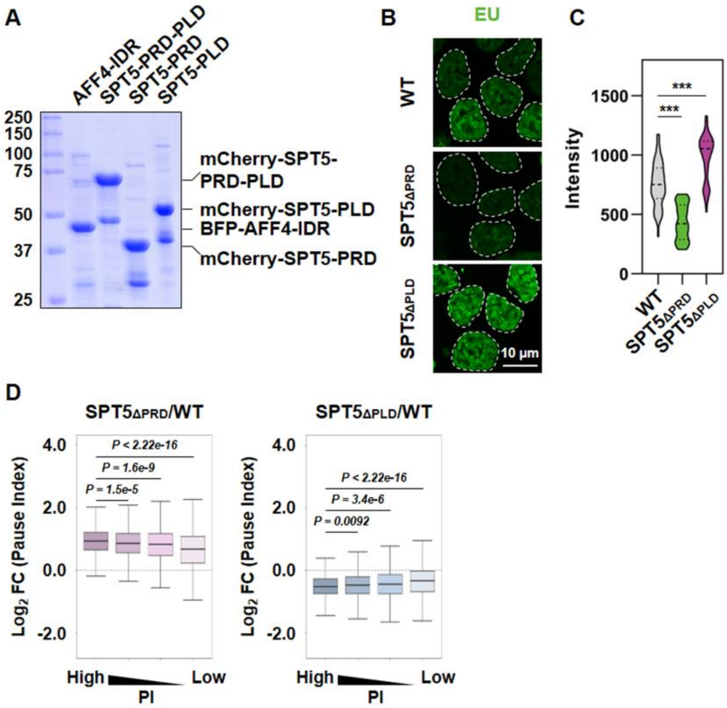

Figure S3. Adjacent PLD and PRD in SPT5 are required for Pol II pausing and elongation respectively.

(A) The recombinant BFP-AFF4-IDR, mCherry-SPT5-PRD-PLD, mCherry-SPT5-PRD, and mCherry-SPT5-PLD proteins were purified, and analyzed by SDS-PAGE followed by Coomassie blue staining. The line represents the purified protein. (B) Confocal imaging of nascent RNA labeled by EU in WT, $SPT5_{\Delta PRD}$, and $SPT5_{\Delta PLD}$ HCT 116 cells. (C) Violin plot showing the intensity of cells in Figure S3B. Results are representative of three biological replicates, each n > 50. Two-tailed, unpaired Student's *t* test was performed. ***p < 0.001. (D) Box plots showing the correlation of log2 FC of Pol II pause index (PI) in four equal groups based on PI of $SPT5_{\Delta PRD}$ (left panel) or $SPT5_{\Delta PLD}$ (right panel) versus WT cells.

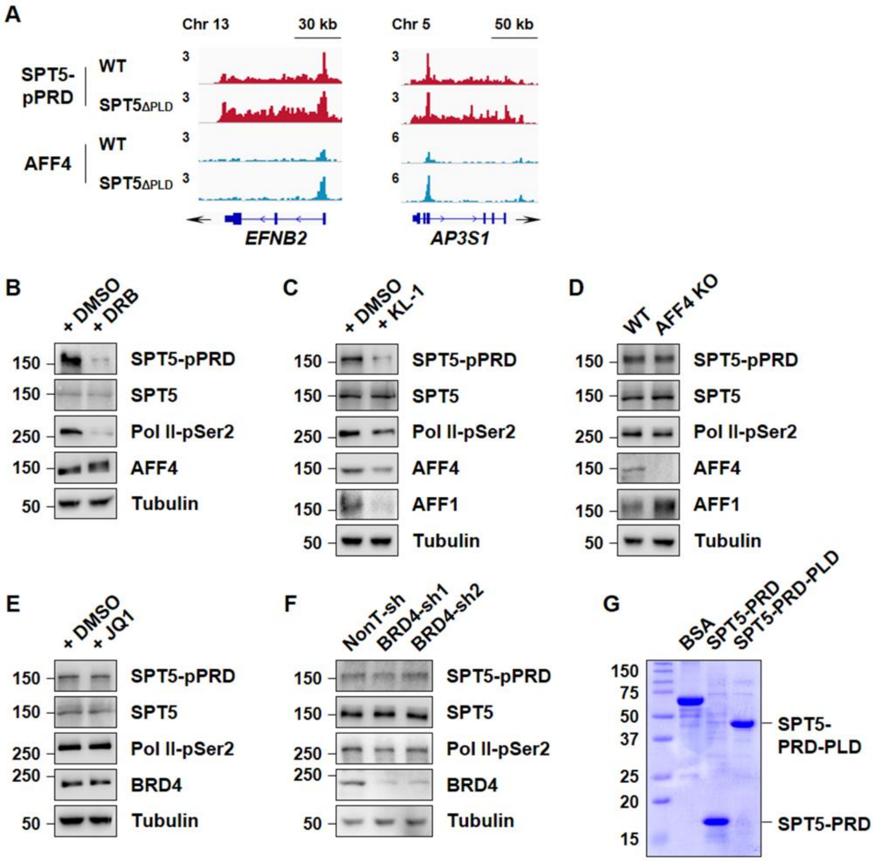

Figure S4. SPT5-PLD inhibits SEC mediated PRD phosphorylation.

(A) Representative gene examples of SPT5-pPRD and AFF4 ChIP-seq in WT and SPT5$_{\Delta PLD}$ HCT 116 cells. Y-axis representing RPM. (B) Western blot analysis of SPT5-pPRD, SPT5, Pol II-pSer2, and AFF4 in HCT 116 cells treated with 3.5 hours DRB (100 μM) or not. (C) Western blot analysis of SPT5-pPRD, SPT5, Pol II-pSer2, AFF4, and AFF1 in HCT 116 cells treated with 6 hours KL-1 (20 μM) or not. (D) Western blot analysis of SPT5-pPRD, SPT5, Pol II-pSer2, AFF4, and AFF1 in WT and AFF4 KO HCT 116 cells. (E) Western blot analysis of SPT5-pPRD, SPT5, Pol II-pSer2, and BRD4 in HCT 116 cells treated with 3 hours JQ1 (1 μM) or not. (F) Western blot analysis of SPT5-pPRD, SPT5, Pol II-pSer2, and BRD4 in HCT 116 cells with knockdown of BRD4. α-Tubulin was used as a loading control. (G) The recombinant SPT5-PRD and SPT5-PRD-PLD proteins were purified, and analyzed by SDS-PAGE followed by Coomassie blue staining. The line represents the purified protein.

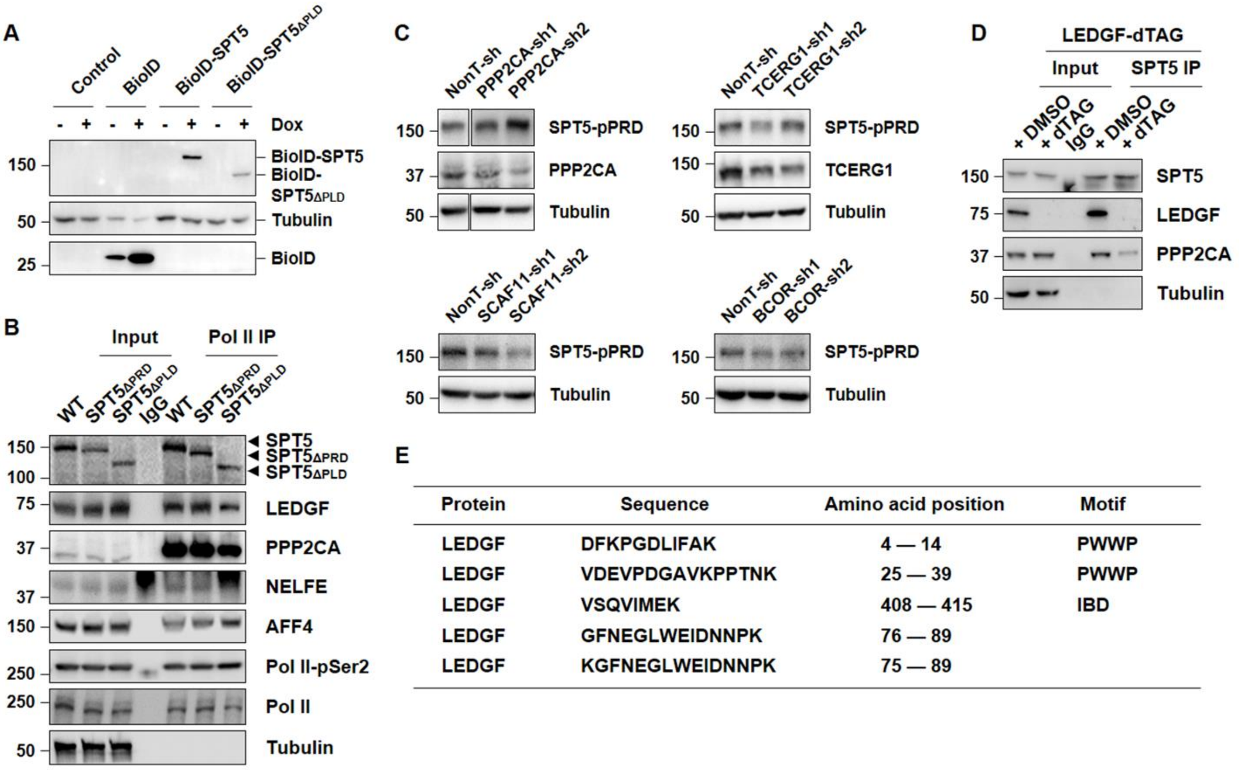

Protein	Sequence	Amino acid position	Motif
LEDGF	DFKPGDLIFAK	4 — 14	PWWP
LEDGF	VDEVPDGAVKPPTNK	25 — 39	PWWP
LEDGF	VSQVIMEK	408 — 415	IBD
LEDGF	GFNEGLWEIDNNPK	76 — 89	
LEDGF	KGFNEGLWEIDNNPK	75 — 89	

Figure S5. LEDGF interacts with SPT5 at PLD.

(A) Generation of BioID tagged proximity labelling FLAG-BioID-SPT5 or -SPT5$_{\Delta PLD}$ cell lines. (B) Endogenous IPs showing the interaction among Pol II and SPT5, LEDGF, PPP2CA, NELFE, AFF4 or Pol II-pSer2 in WT, SPT5$_{\Delta PRD}$, and SPT5$_{\Delta PLD}$ HCT 116 cells. α-Tubulin was used as a control. (C) Western blot analysis of SPT5-pPRD in HCT 116 cells with knockdown of PPP2CA (left-top panel), TCERG1 (right-top panel), SCAF11 (left-bottom panel), or BCOR (right-bottom panel) by independent shRNAs. NonT represents non-target. α-Tubulin was used as a loading control. (D) Endogenous IPs showing the interaction among LEDGF, PPP2CA and SPT5 in LEDGF-dTAG HCT 116 cells treated with dTAG for 3 hours or not. (E) Peptide sequence and motifs associated with LEDGF were analyzed in mass spectrometry.

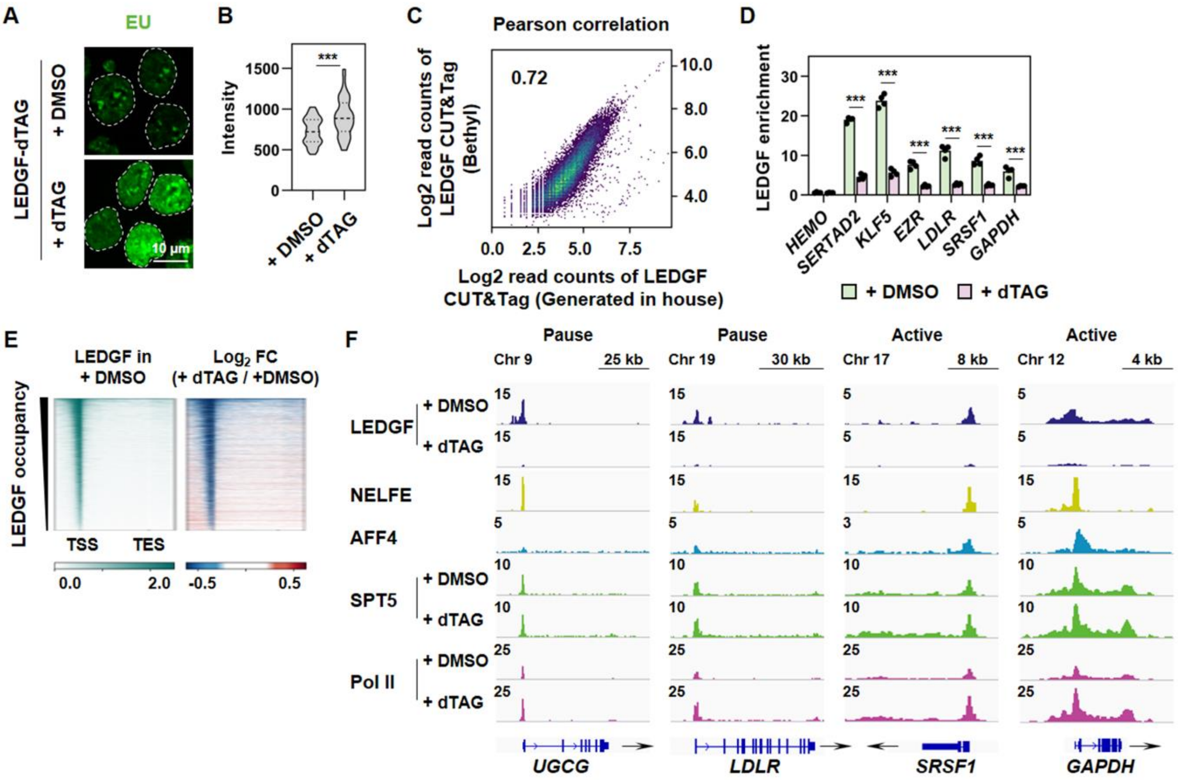

Figure S6. Rapid degradation of LEDGF leads to increased initiating and elongating Pol II.

(A) Confocal imaging of nascent RNA labeled by EU in LEDGF-dTAG HCT 116 cells treated with 3 hours dTAG or not. (B) Violin plot showing the intensity of cells in Figure S6A. Results are representative of three biological replicates, each n > 50. Two-tailed, unpaired Student's *t* test was performed. ***p < 0.001. (C) Scatter plots comparing LEDGF CUT&Tag using two different antibodies to recognize LEDGF/p75 CTD (Bethyl) or IBD (generated-in-house) in HCT 116 cells with Pearson correlation coefficients. (D) LEDGF CUT&Tag-qPCR analysis of example genes in in LEDGF-dTAG HCT 116 cells treated with 3 hours dTAG or not. The *HEMO* gene serves as a negative control. Two-tailed, unpaired Student's *t* test was performed. ***p < 0.001. (E) Heatmaps of LEDGF occupancy showing RPM and log2 FC on scaled genes ranked by decreasing occupancy in LEDGF-dTAG HCT 116 cells treated with 3 hours dTAG or not. N= 6732 genes. (F) Representative gene examples of NELFE, AFF4 ChIP-seq in HCT 116 cells, and SPT5, Pol II ChIP-seq, or LEDGF CUT&Tag in LEDGF-dTAG HCT 116 cells treated with 3 hours dTAG or not were analyzed. Y-axis representing RPM.

Figure S7.

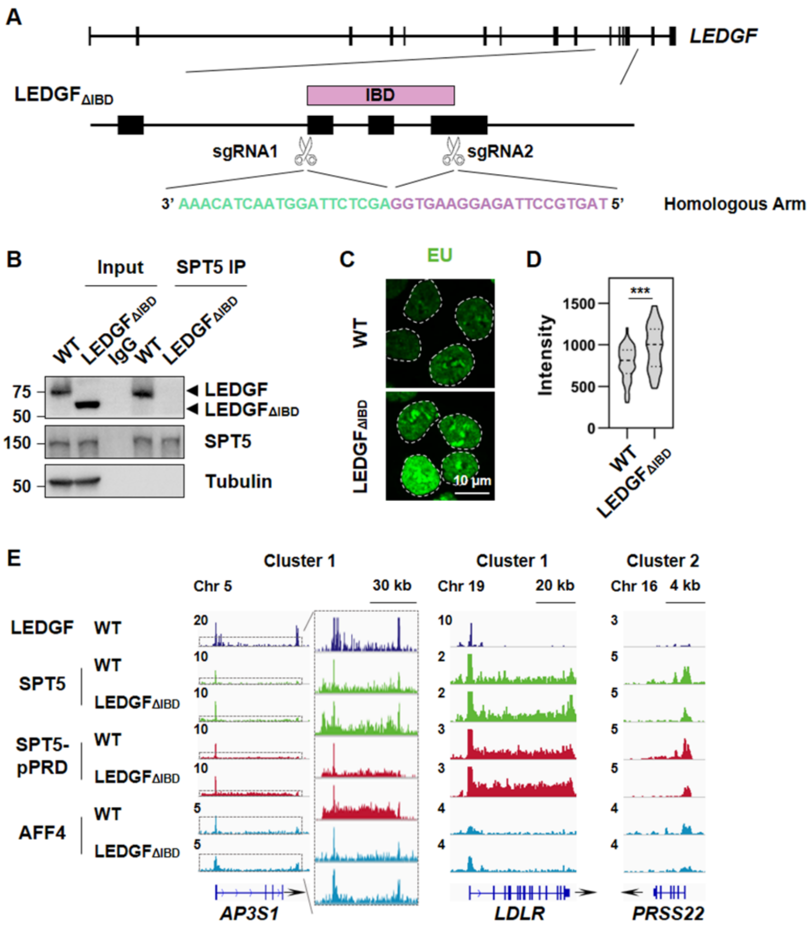

Figure S7. LEDGF/p75 promotes transcriptional pausing at large subset of genes. (A) Schematic representation of the positions of the sgRNAs and homologous templates used to deletion of LEDGF-IBD. (B) Endogenous IPs showing the interaction among LEDGF and SPT5 in WT and $LEDGF_{\Delta IBD}$ HCT 116 cells. (C) Confocal imaging of nascent RNA labeled by EU in WT and $LEDGF_{\Delta IBD}$ HCT 116 cells. (D) Violin plot showing the intensity of cells in Figure S7C. Results are representative of three biological replicates, each $n > 50$. Two-tailed, unpaired Student's *t* test was performed. ***$p < 0.001$. (E) Representative gene examples of LEDGF, SPT5, SPT5-pPRD, and AFF4 ChIP-seq were analyzed in two clusters within both WT and $LEDGF_{\Delta IBD}$ HCT 116 cells. Y-axis representing RPM.

Figure S8.

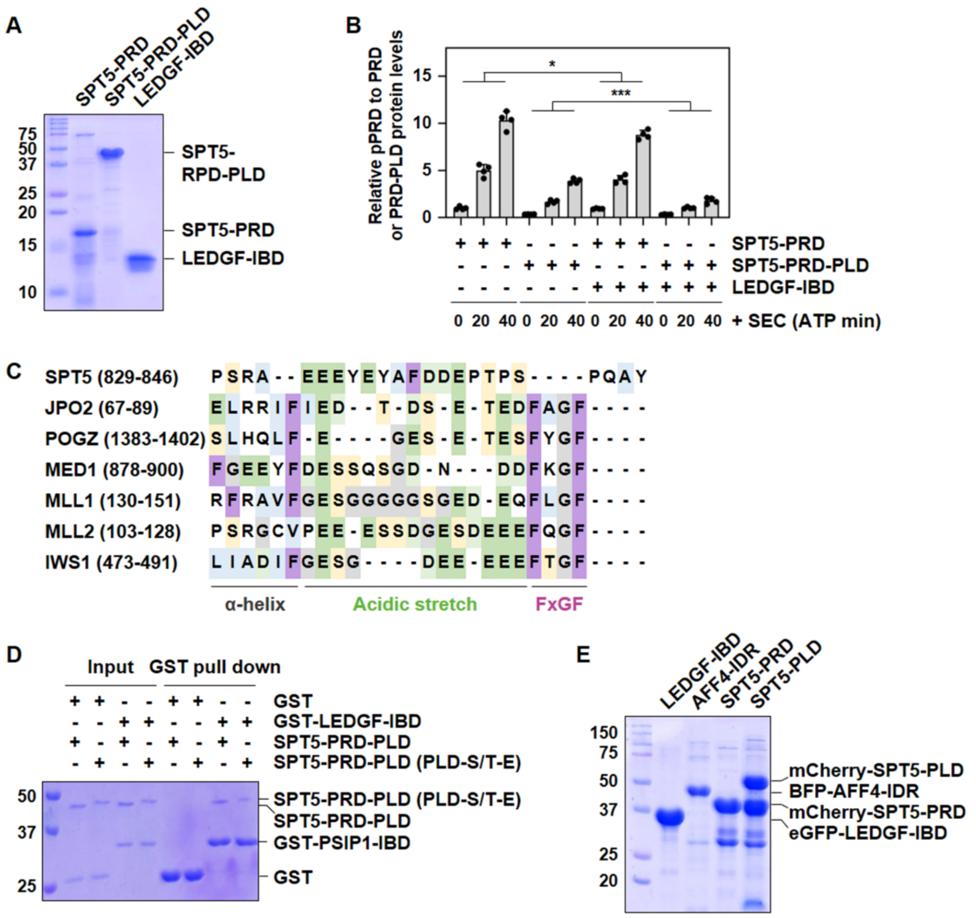

Figure S8. LEDGF-IBD prevents SPT5-PRD phosphorylation by SEC.

(A) The recombinant SPT5-PRD, SPT5-PRD-PLD, and LEDGF-IBD proteins were purified, and analyzed by SDS-PAGE followed by Coomassie blue staining. The line represents the purified protein. (B) Quantification of relative density of SPT5-pPRD compared to SPT5-PRD or SPT5-PRD-PLD in Figure 7A, n = 4. Two-tailed, unpaired Student's *t* test was performed. *$p < 0.05$, ***$p < 0.001$. (C) The LEDGF IBD-binding motifs (IBMs) can be characterized by a region with α-helical propensity followed by an acidic stretch and contain an FxGF motif or not. (D) *In vitro* pull-down assays using purified SPT5-PRD or SPT5-PRD-PLD incubated with GST or GST-LEDGF-IBD first, followed by GST pull down, and analyzed by SDS-PAGE followed by Western blotting or Coomassie blue staining. (E) *In vitro* pull-down assays using purified SPT5-PRD-PLD or SPT5-PRD-PLD (PLD-S/T-E) incubated with GST or GST-LEDGF-IBD first, followed by GST pull down, and analyzed by SDS-PAGE followed by Coomassie blue staining. (F) The recombinant mCherry-SPT5-PRD, mCherry-SPT5-PLD, eGFP-LEDGF-IBD, and BFP-AFF4-IDR proteins were purified, and analyzed by SDS-PAGE followed by Coomassie blue staining. The line represents the purified protein.

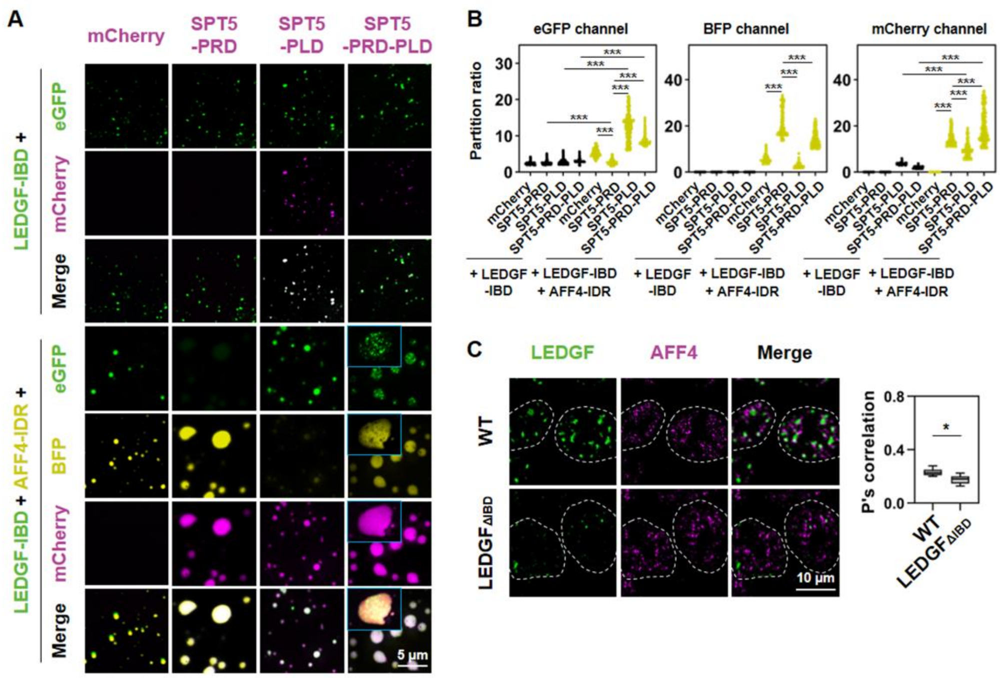

Figure S9. LEDGF-IBD and SEC form distinct condensates with SPT5.

(A) Fluorescence microscopy images showing individual- and co-phase-separated droplets formed in the presence of 10% PEG-8000 with 150 mM NaCl containing buffer and 2 μM eGFP-LEDGF-IBD and BFP-AFF4-IDR along with mCherry, mCherry-SPT5-PRD, mCherry-SPT5-PLD, or mCherry-SPT5-PRD-PLD. (B) Dot plot showing the partition ration in Figure S9A. Fields per condition n = 5. Two-tailed, unpaired Student's *t* test was performed. ***p < 0.001. (C) Confocal images (left panel) showing co-localization of AFF4 with LEDGF in nuclear puncta in WT and $LEDGF_{\Delta IBD}$ HCT 116 cells. Box plots (right panel) showing the mean values of the Pearson correlation coefficient of co-localization ratios of LEDGF with AFF4. Results are representative of three biological replicates, each n > 20. Two-tailed, unpaired Student's *t* test was performed. *p < 0.05.

Table S1. List of key resources used in the study.

REAGENT or RESOURCE	SOURCE	IDENTIFIER
Antibodies		
AFF4	Lin et al., 2010 (*49*)	N/A
AFF4	Santa Cruz Biotechnology	Cat.#sc-390310; RRID: AB_2924396
AFF1	Che et al., 2024 (*57*)	N/A
BRD4	Francisco et al., 2017 (*52*)	N/A
CDK9	Lin et al., 2010 (*49*)	N/A
SPT5	Santa Cruz Biotechnology	Cat.#sc-28678; RRID: AB_668824
SPT5	Santa Cruz Biotechnology	Cat.#sc-133217; RRID: AB_2196394
SPT5	Santa Cruz Biotechnology	Cat.#sc-133097; RRID: AB_1568824
SPT5	Abclonal	Cat.#A9193; RRID: AB_2772472
SPT5	Guo et al., 2023 (*23*)	N/A
SPT5-pPRD	Hu et al., 2021 (*20*)	N/A
SPT5-pS666	Hu et al., 2021 (*20*)	N/A
NELFE	Santa Cruz Biotechnology	Cat.#sc-32912; RRID: AB_2177858
NELFE	Santa Cruz Biotechnology	Cat.#sc-377052; RRID: AB_2847957
NELFE	Guo et al., 2023 (*23*)	N/A
Pol II	Santa Cruz Biotechnology	N20
PAF1	Abcam	Cat.#ab20662; RRID: AB_2159769
PP2A	Abclonal	Cat.#A6702; RRID: AB_2767286
LEDGF	Abclonal	Cat.#A18101; RRID: AB_2861895
LEDGF	Abcam	Cat.#ab177159; RRID: N/A
LEDGF	Bethyl Laboratories	Cat.#A300-848A; RRID: AB_2171223
LEDGF	This Paper	N/A
TCERG1	Proteintech	Cat.#21858-1-AP; RRID: AB_11183756

RNA polymerase II CTD repeat YSPTSPS (phospho S5)	Abcam	Cat.#ab232852; RRID: N/A
Phospho-POLR2A-S5 Rabbit pAb	Abclonal	Cat.#AP0828; RRID: AB_2771442
RNA polymerase II CTD repeat YSPTSPS (phospho S2)	Abcam	Cat.#ab238146; RRID: N/A
α-Tubulin	Abcam	Cat.#ab7291; RRID: AB_2241126
FLAG	Sigma-Aldrich	Cat.#F1804; RRID: AB_262044
MYC-TAG	Abclonal	Cat.#AE010; RRID: AB_2770408
HRP Anti-Streptavidin	Abcam	Cat.#ab191338; RRID: N/A
Goat anti-Rabbit IgG Alexa Fluor 488	Life Technologies	Cat.#A11070; RRID: AB_2534114
Goat anti-Mouse IgG Alexa Fluor 488	Life Technologies	Cat.#A10684; RRID: AB_2534064
Goat anti-Rabbit IgG Alexa Fluor 647	Abcam	Cat.#ab150083; RRID: AB_2714032
Bacterial strain		
BL21		N/A
Chemicals, peptides, and recombinant proteins		
Proteinase K	Thermo Fisher Scientific	Cat.#25530049
Ribonuclease A	Sigma-Aldrich	Cat.#R6513
Pierce Universal Nuclease	Vazyme	Cat.#DD4301-PC
1,6-hexanediol	Sigma-Aldrich	Cat.#240117
PEG-8000	Sangon Biotech	Cat.#A100159
JQ1	Sigma-Aldrich	Cat.#SML0974
Flavopiridol	MedChemExpress	Cat.#HY-10005
DRB	Sigma-Aldrich	Cat.#D1916
SEC inhibitor KL-1	MedChemExpress	Cat.#HY-122720
Critical commercial reagents		
Ni-NTA Agarose	QIAGEN	Cat.#30210
Protein A Agarose	Santa Cruz	Cat.#sc-2001
Glutathione Beads	Smart-Lifesciences	Cat.#SEA008010
Gelatin Sepharose Beads	Smart-Lifesciences	Cat.#SEC0061
FOS DNA FISH probe	Empire Genomics	N/A
FastPure Gel DNA Extraction Mini Kit	Vazyme	Cat.#DC301-01

VAHTS Universal DNA Library Prep Kit for Illumina V3	Vazyme	Cat.#ND607-02
VAHTS DNA Adapters set1 for Illumina	Vazyme	Cat.#N801-02
Hyperactive Universal CUT&Tag Assay Kit for Illumina Pro	Vazyme	Cat.#TD904
TruePrep Index Kit V2 for Illumina	Vazyme	Cat.#TD202
Deposited data		
Raw and analyzed data	This paper	GEO: GSE250380
Experimental models: Cell lines		
HCT 116	ATCC	ATCC® CCL-247™
HCT 116 AFF4 KO	Che et al., 2024 (*57*)	N/A
HCT 116 $SPT5_{\Delta PRD}$	This Paper	N/A
HCT 116 $SPT5_{\Delta PLD}$	This Paper	N/A
HCT 116 LEDGF-dTAG	This Paper	N/A
HCT 116 $LEDGF_{\Delta IBD}$	This Paper	N/A
HEK293 Flp-In TRex	Invitrogen	Cat.#R78007
HEK293 FLAG-BioID-SPT5	This Paper	N/A
HEK293 FLAG-BioID-$SPT5_{\Delta PLD}$	This Paper	N/A
Recombinant DNA		
pET16b-SPT5-PRD	This Paper	N/A
pET16b-SPT5-RPD-PLD	This Paper	N/A
pET16b-SPT5-PRD-PLD (PLD-S/T-E)	This Paper	N/A
pET16b-LEDGF-IBD	This Paper	N/A
pET16b-mCherry-SPT5-PRD-PLD	Guo et al., 2023 (*23*)	N/A
pET16b-mCherry-SPT5-PRD	This Paper	N/A
pET16b-mCherry-SPT5-PLD	This Paper	N/A
pET16b-BFP-AFF4-IDR	Guo et al., 2023 (*23*)	N/A
pET16b-eGFP-LEDGF-IBD	This Paper	N/A
pGEX-5X-1-LEDGF-IBD	This Paper	N/A
pcDNA5-FLAG-AFF4	Lin et al., 2010 (*49*)	N/A
pcDNA5-FLAG-SPT5	This Paper	N/A
pcDNA5-MYC-LEDGF	This Paper	N/A

pcDNA5-MYC-LEDGF$_{\Delta PWWP}$	This Paper	N/A
pcDNA5-MYC-LEDGF$_{\Delta IBD}$	This Paper	N/A
lentiCRISPR v2-SPT5-sgRNA-1	This Paper	N/A
lentiCRISPR v2-SPT5-sgRNA-2	This Paper	N/A
lentiCRISPR v2-SPT5-sgRNA-3	This Paper	N/A
lentiCRISPR v2-SPT5-sgRNA-4	This Paper	N/A
pX459-LEDGF-sgRNA	This Paper	N/A
pX459-LEDGF-sgRNA1	This Paper	N/A
pX459-LEDGF-sgRNA2	This Paper	N/A
pX459 PITCh sgRNA	Hu et al., 2021 (*20*)	N/A
pUC57 PITCh SPT5-HR1	This Paper	N/A
pUC57 PITCh SPT5-HR2	This Paper	N/A
pUC57 PITCh LEDGF-HR	This Paper	N/A
Software and Algorithms		
FIJI	Schindelin et al., 2012 (*50*)	https://imagej.net/Fiji
SAMtools v1.15.1	Li et al., 2009 (*58*)	http://samtools.sourceforge.net
Bedtools v2.30.0	Quinlan and Hall, 2010 (*59*)	https://bedtools.readthedocs.io/en/latest/
Trim Galore v0.6.7	N/A	https://www.bioinformatics.babraham.ac.uk/projects/trim_galore/
Bowtie v2.4.5	Langmead and Salzberg, 2012 (*53*)	http://bowtie-bio.sourceforge.net/bowtie2/index.shtml
deepTools v 3.5.1	Ramírez et al., 2016 (*54*)	https://deeptools.readthedocs.io/en/develop/
Picard 2.27.4	N/A	https://broadinstitute.github.io/picard/
MACS 2.2.7.1	Zhang et al., 2008 (*60*)	https://github.com/macs3-project/MACS
ChIPseeker R package v1.30.3	Yu et al., 2015 (*55*)	https://bioconductor.org/packages/release/bioc/html/ChIPseeker.html

Table S2. List of oligonucleotides used in the study.

Oligonucleotides used for sgRNAs		
Name	**Description**	**Sequence (5'-3')**
SPT5 sgRNA-1	guide RNA targeting SPT5 locus	GGACCGTCAGCGGCTCACCA
SPT5 sgRNA-2	guide RNA targeting SPT5 locus	ACAACCCCAACACGCCGTCA
SPT5 sgRNA-3	guide RNA targeting SPT5 locus	TATTCTTCCTCAGCCCTGTT
SPT5 sgRNA-4	guide RNA targeting SPT5 locus	GTTTAGGGGGTACCAAGGAG
LEDGF sgRNA	guide RNA targeting LEDGF locus	TGAAATCGCGAGTCATGTTT
LEDGF sgRNA1	guide RNA targeting LEDGF locus	CAATGGATTCTCGACTTCAA
LEDGF sgRNA2	guide RNA targeting LEDGF locus	CAAAGTTAGTCAGGTAATCA
Primers used for genotyping		
Name	**Description**	**Sequence (5'-3')**
$SPT5_{\Delta PRD}$-F	Genotyping	AGTGACATTCTCCCCAATCCC
$SPT5_{\Delta PRD}$-R1	Genotyping	AGAGAACTGGTCTGTGTTGTACC
$SPT5_{\Delta PRD}$-R2	Genotyping	CCATACATGGGCGTCCTCC
$SPT5_{\Delta PLD}$-F	Genotyping	AGTGACATTCTCCCCAATCCC
$SPT5_{\Delta PLD}$-R1	Genotyping	GGGACAGGTCTGTCTCCAGTTTA
$SPT5_{\Delta PLD}$-R2	Genotyping	AGAGAACTGGTCTGTGTTGTACC
LEDGF-dTAG-F	Genotyping	TTCGCTTTAACCGCCCTC
LEDGF-dTAG-R	Genotyping	TCTGTCCAAGTCTGCCAATA
$LEDGF_{\Delta IBD}$-F1	Genotyping	GACGCCAAGTGGTGGTTTTG
$LEDGF_{\Delta IBD}$-F2	Genotyping	AGGCCTTGGATGAACTTGCT
$LEDGF_{\Delta IBD}$-R	Genotyping	GCAGTCCTGGCAAATGGTTT
Oligonucleotides used for HR arm		
Name	**Description**	**Sequence (5'-3')**
SPT5-PITCh-HR1	HR for $SPT5_{\Delta PRD}$	GGAACCCTGGACTCACCGTGACGGGAGCCGCTGACGGTCCACAGAGAT
SPT5-PITCh-HR2	HR for $SPT5_{\Delta PLD}$	TGTCTCCAGTTTAGGGGGTACCAATGTTGAAAGAAAAGTCTGTTGACA

LEDGF-PITCh-HR1	HR for LEDGF-dTAG	CCCGGTCTCGCCCCCGAAAC-Puro-P2A-Flag-Fkbp12^{F36V}-ACTCGCGATTTCAAACCTGG
LEDGF-HR	HR for LEDGF$_{\Delta IBD}$	AAACATCAATGGATTCTCGAG GTGAAGGAGATTCCGTGAT
Oligonucleotides used for shRNAs		
Name	**Description**	**Sequence (5'-3')**
LEDGF shRNA1	RNAi mediated LEDGF knockdown	GCAGCAACTAAACAATCAAA T
LEDGF shRNA2	RNAi mediated LEDGF knockdown	GCAGCTACAGAAGTCAAGAT T
PPP2CA shRNA1	RNAi mediated PPP2CA knockdown	TGGAACTTGACGATACTCTAA
PPP2CA shRNA2	RNAi mediated PPP2CA knockdown	CCCATGTTGTTCTTTGTTATT
TCERG1 shRNA1	RNAi mediated TCERG1 knockdown	CCACGTTACAAAGCAGTAGA T
TCERG1 shRNA2	RNAi mediated TCERG1 knockdown	CCTCCTATCGTACCCATGATA
BCOR shRNA1	RNAi mediated BCOR knockdown	CCACGAAACTTATACTTTCAA
BCOR shRNA2	RNAi mediated BCOR knockdown	GCTCTATATTTCTGTCTCCAA
SCAF11 shRNA1	RNAi mediated SCAF11 knockdown	GCATTTATTCTGTCAGGTTAA
SCAF11 shRNA2	RNAi mediated SCAF11 knockdown	CATCTGTAAATGCTGATCTTA
Oligonucleotides used for qPCR		
*SERTAD2*_promoter-F	CUT&Tag-qPCR primer	TGGGAACTAACGCATCAGGA
*SERTAD2*_promoter-R	CUT&Tag-qPCR primer	AGAGAACGGCGGAGTCTTAG
*KLF5*_promoter-F	CUT&Tag-qPCR primer	GCCTCTCTCCCTGCTCATAG
*KLF*5_promoter-R	CUT&Tag-qPCR primer	CGACTACTGACACTTGACGC
*EZR*_promoter-F	CUT&Tag-qPCR primer	GCAACTTACTGGTTTCGGCA

*EZR*_promoter-R	CUT&Tag-qPCR primer	AAGGGTTCTGCTCTGACTCC
*LDLR*_promoter-F	CUT&Tag-qPCR primer	TCCCCTTGTCCAATGTGAGG
*LDLR*_promoter-R	CUT&Tag-qPCR primer	AAGGTGAGGCTCAGACTTCC
*SRSF1*_promoter-F	CUT&Tag-qPCR primer	TCGTAGGGTGCGTCTAATCC
*SRSF1*_promoter-R	CUT&Tag-qPCR primer	GTCTAAGCAGCCACGGTCTA

REFERENCES AND NOTES

1. F. X. Chen, E. R. Smith, A. Shilatifard, Born to run: Control of transcription elongation by RNA polymerase II. *Nat. Rev. Mol. Cell. Bio.* **19**, 464–478 (2018).

2. L. Core, K. Adelman, Promoter-proximal pausing of RNA polymerase II: A nexus of gene regulation. *Gene Dev.* **33**, 960–982 (2019).

3. R. Dollinger, D. S. Gilmour, Regulation of promoter proximal pausing of RNA polymerase II in metazoans. *J. Mol. Biol.* **433**, 166897 (2021).

4. C. H. Guo, Z. J. Luo, C. Q. Lin, Dynamic regulation of promoter-proximal RNA polymerase II pausing. *Chin. Sci. B. Chin.* **65**, 4084–4094 (2020).

5. Y. Aoi, A. Shilatifard, Transcriptional elongation control in developmental gene expression, aging, and disease. *Mol. Cell* **83**, 3972–3999 (2023).

6. T. M. Decker, Mechanisms of transcription elongation factor DSIF (Spt4-Spt5). *J. Mol. Biol.* **433**, 166657 (2021).

7. G. A. Hartzog, J. H. Fu, The Spt4-Spt5 complex: A multi-faceted regulator of transcription elongation. *Bba-Gene Regul. Mech.* **1829**, 105–115 (2013).

8. Y. Yamaguchi, H. Shibata, H. Handa, Transcription elongation factors DSIF and NELF: Promoter-proximal pausing and beyond. *Bba-Gene Regul. Mech.* **1829**, 98–104 (2013).

9. B. Cheng, D. H. Price, Properties of RNA polymerase II elongation complexes before and after the P-TEFb-mediated transition into productive elongation. *J. Biol. Chem.* **282**, 21901–21912 (2007).

10. J. B. Kim, P. A. Sharp, Positive transcription elongation factor b phosphorylates hSPT5 and RNA polymerase II carboxyl-terminal domain independently of cyclin-dependent kinase-activating kinase. *J. Biol. Chem.* **276**, 12317–12323 (2001).

11. T. Yamada, Y. Yamaguchi, N. Inukai, S. Okamoto, T. Mura, H. Handa, P-TEFb-mediated phosphorylation of hSpt5 C-terminal repeats is critical for processive transcription elongation. *Mol. Cell* **21**, 227–237 (2006).

12. M. S. Swanson, E. A. Malone, F. Winston, Spt5, an essential gene important for normal transcription in Saccharomyces-cerevisiae, encodes an acidic nuclear-protein with a carboxy terminal repeat. *Mol. Cell. Biol.* **11**, 3009–3019 (1991).

13. T. Wada, T. Takagi, Y. Yamaguchi, A. Ferdous, T. Imai, S. Hirose, S. Sugimoto, K. Yano, G. A. Hartzog, F. Winston, S. Buratowski, H. Handa, DSIF, a novel transcription elongation factor that regulates RNA polymerase II processivity, is composed of human Spt4 and Spt5 homologs. *Gene De.v* **12**, 343–356 (1998).

14. A. X. Song, F. X. Chen, The pleiotropic roles of SPT5 in transcription. *Transcr. Austin.* **13**, 53–69 (2022).

15. F. Werner, A nexus for gene expression-molecular mechanisms of Spt5 and NusG in the three domains of life. *J. Mol. Biol.* **417**, 13–27 (2012).

16. Y. J. Qiu, D. S. Gilmour, Identification of regions in the Spt5 subunit of DRB sensitivity-inducing factor (DSIF) that are involved in promoter-proximal pausing. *J. Biol. Chem.* **292**, 5555–5570 (2017).

17. C. Bernecky, J. M. Plitzko, P. Cramer, Structure of a transcribing RNA polymerase II-DSIF complex reveals a multidentate DNA-RNA clamp. *Nat. Struct. Mol. Biol.* **24**, 809–815 (2017).

18. H. Ehara, T. Yokoyama, H. Shigematsu, S. Yokoyama, M. Shirouzu, S. I. Sekine, Structure of the complete elongation complex of RNA polymerase II with basal factors. *Science* **357**, 921–924 (2017).

19. N. Fong, R. M. Sheridan, S. Ramachandran, D. L. Bentley, The pausing zone and control of RNA polymerase II elongation by Spt5: Implications for the pause-release model. *Mol. Cell* **82**, 3632–3645.e4 (2022).

20. S. B. Hu, L. Peng, C. Xu, Z. Wang, A. Song, F. X. Chen, SPT5 stabilizes RNA polymerase II, orchestrates transcription cycles, and maintains the enhancer landscape. *Mol. Cell* **81**, 4425–4439.e6 (2021).

21. M. Sansó, R. S. Levin, J. J. Lipp, V. Y. F. Wang, A. K. Greifenberg, E. M. Quezada, A. Ali, A. Ghosh, S. Larochelle, T. M. Rana, M. Geyer, L. Tong, K. M. Shokat, R. P. Fisher, P-TEFb regulation of transcription termination factor Xrn2 revealed by a chemical genetic screen for Cdk9 substrates. *Gene Dev.* **30**, 117–131 (2016).

22. Z. J. Luo, C. Q. Lin, A. Shilatifard, The super elongation complex (SEC) family in transcriptional control. *Nat. Rev. Mol. Cell Bio.* **13**, 543–547 (2012).

23. C. H. Guo, Y. Zhang, S. Shuai, A. Sigbessia, S. Hao, P. Xie, X. Jiang, Z. Luo, C. Lin, The super elongation complex (SEC) mediates phase transition of SPT5 during transcriptional pause release. *EMBO Rep.* **24**, e55699 (2023).

24. H. Ge, Y. Z. Si, R. G. Roeder, Isolation of cDNAs encoding novel transcription coactivators p52 and p75 reveals an alternate regulatory mechanism of transcriptional activation. *EMBO J.* **17**, 6723–6729 (1998).

25. D. P. Singh, A. Kimura, L. T. Chylack, T. Shinohara, Lens epithelium-derived growth factor (LEDGF/p75) and p52 are derived from a single gene by alternative splicing. *Gene* **242**, 265–273 (2000).

26. R. van Nuland, F. M. A. van Schaik, M. Simonis, S. van Heesch, E. Cuppen, R. Boelens, H. T. M. Timmers, H. van Ingen, Nucleosomal DNA binding drives the recognition of H3K36-methylated nucleosomes by the PSIP1-PWWP domain. *Epigenetics Chromatin* **6**, 12 (2013).

27. A. Basu, T. W. Sanchez, C. A. Casiano, DFS70/LEDGFp75: An enigmatic autoantigen at the interface between autoimmunity, AIDS and cancer. *Front. Immunol.* **6**, 1–5 (2015).

28. A. K. Chakravarty, D. F. Jarosz, More than just a phase: Prions at the crossroads of epigenetic inheritance and evolutionary change. *J. Mol. Biol.* **430**, 4607–4618 (2018).

29. C. H. Guo, Z. Che, J. Yue, P. Xie, S. Hao, W. Xie, Z. Luo, C. Lin, ENL initiates multivalent phase separation of the super elongation complex (SEC) in controlling rapid transcriptional activation. *Sci. Adv.* **6**, eaay4858 (2020).

30. K. J. Roux, D. I. Kim, M. Raida, B. Burke, A promiscuous biotin ligase fusion protein identifies proximal and interacting proteins in mammalian cells. *J. Cell Biol.* **196**, 801–810 (2012).

31. L. M. Appel, V. Franke, J. Benedum, I. Grishkovskaya, X. Strobl, A. Polyansky, G. Ammann, S. Platzer, A. Neudolt, A. Wunder, L. Walch, S. Kaiser, B. Zagrovic, K. Djinovic-Carugo, A. Akalin, D. Slade, The SPOC domain is a phosphoserine binding module that bridges transcription machinery with co- and post-transcriptional regulators. *Nat. Commun.* **14**, 166 (2023).

32. M. B. Ardehali, M. Damle, C. Perea-Resa, M. D. Blower, R. E. Kingston, Elongin A associates with actively transcribed genes and modulates enhancer RNA levels with limited impact on transcription elongation rate. *J. Biol. Chem.* **296**, 100202 (2021).

33. C. C. Ebmeier, B. Erickson, B. L. Allen, M. A. Allen, H. Kim, N. Fong, J. R. Jacobsen, K. Liang, A. Shilatifard, R. D. Dowell, W. M. Old, D. L. Bentley, D. J. Taatjes, Human TFIIH Kinase CDK7 regulates transcription-associated chromatin modifications. *Cell Rep.* **20**, 1173–1186 (2017).

34. S. Bhattacharya, M. J. Levy, N. Zhang, H. Li, L. Florens, M. P. Washburn, J. L. Workman, The methyltransferase SETD2 couples transcription and splicing by engaging mRNA processing factors through its SHI domain. *Nat. Commun.* **12**, 1443 (2021).

35. K. L. Huang, D. Jee, C. B. Stein, N. D. Elrod, T. Henriques, L. G. Mascibroda, D. Baillat, W. K. Russell, K. Adelman, E. J. Wagner, Integrator recruits protein phosphatase 2A to prevent pause release and facilitate transcription termination. *Mol. Cell* **80**, 345–358.e9 (2020).

36. B. Nabet, J. M. Roberts, D. L. Buckley, J. Paulk, S. Dastjerdi, A. Yang, A. L. Leggett, M. A. Erb, M. A. Lawlor, A. Souza, T. G. Scott, S. Vittori, J. A. Perry, J. Qi, G. E. Winter, K. K. Wong, N. S. Gray, J. E. Bradner, The dTAG system for immediate and target-specific protein degradation. *Nat. Chem. Biol.* **14**, 431–441 (2018).

37. K. Cermakova, J. Demeulemeester, V. Lux, M. Nedomova, S. R. Goldman, E. A. Smith, P. Srb, R. Hexnerova, M. Fabry, M. Madlikova, M. Horejsi, J. de Rijck, Z. Debyser, K. Adelman, H. C. Hodges, V. Veverka, A ubiquitous disordered protein interaction module orchestrates transcription elongation. *Science* **374**, 1113–1121 (2021).

38. S. Sharma, K. Čermáková, J. de Rijck, J. Demeulemeester, M. Fábry, S. el Ashkar, S. van Belle, M. Lepšík, P. Tesina, V. Duchoslav, P. Novák, M. Hubálek, P. Srb, F. Christ, P. Řezáčová, H. C. Hodges, Z. Debyser, V. Veverka, Affinity switching of the LEDGF/p75 IBD interactome is governed by kinase-dependent phosphorylation. *Proc. Natl. Acad. Sci. U.S.A.* **115**, E7053–E7062 (2018).

39. S. Jayakumar, M. Patel, F. Boulet, H. Aziz, G. N. Brooke, H. Tummala, M. M. Pradeepa, PSIP1/LEDGF reduces R-loops at transcription sites to maintain genome integrity. *Nat. Commun.* **15**, 361 (2024).

40. E. Koutná, V. Lux, T. Kouba, J. Škerlová, J. Nováček, P. Srb, R. Hexnerová, H. Šváchová, Z. Kukačka, P. Novák, M. Fábry, S. Poepsel, V. Veverka, Multivalency of nucleosome recognition by LEDGF. *Nucleic Acids Res.* **51**, 10011–10025 (2023).

41. G. LeRoy, O. Oksuz, N. Descostes, Y. Aoi, R. A. Ganai, H. O. Kara, J. R. Yu, C. H. Lee, J. Stafford, A. Shilatifard, D. Reinberg, LEDGF and HDGF2 relieve the nucleosome-induced barrier to transcription in differentiated cells. *Sci. Adv.* **5**, eaay3068 (2019).

42. H. Zheng, Y. Qi, S. Hu, X. Cao, C. Xu, Z. Yin, X. Chen, Y. Li, W. Liu, J. Li, J. Wang, G. Wei, K. Liang, F. X. Chen, Y. Xu, Identification of Integrator-PP2A complex (INTAC), an RNA polymerase II phosphatase. *Science* **370**, eabb5872 (2020).

43. C. L. Xu, C. Li, J. Chen, Y. Xiong, Z. Qiao, P. Fan, C. Li, S. Ma, J. Liu, A. Song, B. Tao, T. Xu, W. Xu, Y. Chi, J. Xue, P. Wang, D. Ye, H. Gu, P. Zhang, Q. Wang, R. Xiao, J. Cheng, H. Zheng, X. Yu, Z. Zhang, J. Wu, K. Liang, Y.-J. Liu, H. Lu, F. X. Chen, R-loop-dependent promoter-proximal termination ensures genome stability. *Nature* **621**, 610–619 (2023).

44. S. B. Hu, L. Peng, A. Song, Y.-X. Ji, J. Cheng, M. Wang, F. X. Chen, INTAC endonuclease and phosphatase modules differentially regulate transcription by RNA polymerase II. *Mol. Cell* **83**, 1588–1604.e5 (2023).

45. R. Fujiwara, S. N. Zhai, D. Liang, A. P. Shah, M. Tracey, X. K. Ma, C. J. Fields, M. S. Mendoza-Figueroa, M. C. Meline, D. C. Tatomer, L. Yang, J. E. Wilusz, IntS6 and the integrator phosphatase module tune the efficiency of select premature transcription termination events. *Mol. Cell* **83**, 4445–4460.e7 (2023).

46. S. Larochelle, J. Batliner, M. J. Gamble, N. M. Barboza, B. C. Kraybill, J. D. Blethrow, K. M. Shokat, R. P. Fisher, Dichotomous but stringent substrate selection by the dual-function Cdk7 complex revealed by chemical genetics. *Nat. Struct. Mol. Biol.* **13**, 55–62 (2006).

47. T. Sakuma, S. Nakade, Y. Sakane, K. T. Suzuki, T. Yamamoto, MMEJ-assisted gene knock-in using TALENs and CRISPR-Cas9 with the PITCh systems. *Nat. Protoc.* **11**, 118–133 (2016).

48. R. M. Sears, D. G. May, K. J. Roux, BioID as a tool for protein-proximity labeling in living cells. *Methods Mol. Biol.* **2012**, 299–313 (2019).

49. C. Lin, E. R. Smith, H. Takahashi, K. C. Lai, S. Martin-Brown, L. Florens, M. P. Washburn, J. W. Conaway, R. C. Conaway, A. Shilatifard, AFF4, a component of the ELL/P-TEFb elongation complex and a shared subunit of MLL chimeras, can link transcription elongation to leukemia. *Mol. Cell* **37**, 429–437 (2010).

50. J. Schindelin, I. Arganda-Carreras, E. Frise, V. Kaynig, M. Longair, T. Pietzsch, S. Preibisch, C. Rueden, S. Saalfeld, B. Schmid, J.Y. Tinevez, D. J. White, V. Hartenstein, K. Eliceiri, P. Tomancak, A. Cardona, Fiji: An open-source platform for biological-image analysis. *Nat. Methods* **9**, 676–682 (2012).

51. C. Y. Jao, A. Salic, Exploring RNA transcription and turnover in vivo by using click chemistry. *Proc. Natl. Acad. Sci. U.S.A.* **105**, 15779–15784 (2008).

52. J. C. Francisco, Q. Dai, Z. Luo, Y. Wang, R. H. H. Chong, Y. J. Tan, W. Xie, G. H. Lee, C. Lin, Transcriptional elongation control of hepatitis B virus covalently closed circular DNA transcription by super elongation complex and BRD4. *Mol. Cell. Biol.* **37**, e00040-17 (2017).

53. B. Langmead, S. L. Salzberg, Fast gapped-read alignment with Bowtie 2. *Nat. Methods* **9**, 357–359 (2012).

54. F. Ramirez, D. P. Ryan, B. Grüning, V. Bhardwaj, F. Kilpert, A. S. Richter, S. Heyne, F. Dündar, T. Manke, deepTools2: A next generation web server for deep-sequencing data analysis. *Nucleic Acids Res.* **44**, W160–W165 (2016).

55. G. C. Yu, L. G. Wang, Q. Y. He, ChIPseeker: An R/Bioconductor package for ChIP peak annotation, comparison and visualization. *Bioinformatics* **31**, 2382–2383 (2015).

56. A. K. Lancaster, A. Nutter-Upham, S. Lindquist, O. D. King, PLAAC: A web and command-line application to identify proteins with prion-like amino acid composition. *Bioinformatics* **30**, 2501–2502 (2014).

57. Z. Z. Che, X. Liu, Q. Dai, K. Fang, C. Guo, J. Yue, H. Fang, P. Xie, Z. Luo, C. Lin,, Distinct roles of two SEC scaffold proteins, AFF1 and AFF4, in regulating RNA polymerase II transcription elongation. *J. Mol. Cell Biol.* **15**, mjad049 (2024).

58. H. Li, B. Handsaker, A. Wysoker, T. Fennell, J. Ruan, N. Homer, G. Marth, G. Abecasis, R. Durbin; 1000 Genome Project Data Processing Subgroup, The sequence alignment/map format and SAMtools. *Bioinformatics* **25**, 2078–2079 (2009).

59. A. R. Quinlan, I. M. Hall, BEDTools: A flexible suite of utilities for comparing genomic features. *Bioinformatics* **26**, 841–842 (2010).

60. Y. Zhang, T. Liu, C. A. Meyer, J. Eeckhoute, D. S. Johnson, B. E. Bernstein, C. Nusbaum, R. M. Myers, M. Brown, W. Li, X. S. Liu, Model-based analysis of ChIP-Seq (MACS). *Genome Biol.* **9**, R137 (2008).